JOURNAL OF
Materials
CHEMISTRY

Solvent-free synthesis of binary inorganic oxides

John N. Hay*† and Hema M. Raval

Department of Chemistry, School of Physical Sciences, University of Surrey, Guildford, Surrey, UK GU2 5XH

The non-hydrolytic sol–gel route has been used in the solvent-free synthesis of binary inorganic oxides based on silicon, aluminium and titanium. Where necessary, iron(III) chloride was used as a catalyst. Clear evidence for the formation of true, amorphous binary systems was obtained only in the case of aluminosilicates. A crystalline aluminosilicate was obtained after calcination at 1000 °C. A titanium–silicon binary system gave only crystalline rutile and anatase following calcination, with no evidence for either crystalline silica or a binary oxide.

Low temperature routes to inorganic oxides have attracted considerable attention in recent years owing to their reduced energy demand compared to traditional high temperature glass forming processes and the potential opened up for combining the oxides with thermally labile organic compounds. The oxides and their hybrids have a plethora of uses, including catalysis and catalyst supports, ceramics, sensor applications and active glasses. The most important synthetic route is the hydrolytic sol–gel method which allows inorganic oxides and/or their immediate precursors to be produced from simple alkoxides or chelates *via* low temperature hydrolysis and condensation reactions. This route has fairly widespread applicability and has been the subject of a number of recent books and reviews.[1–7] For certain applications, however, this approach has a number of disadvantages, including the need to add water for the hydrolysis, the formation of condensation by-products (*e.g.* water, alcohols) and the initial formation of a solvent-swollen gel which undergoes substantial shrinkage on drying. In addition, for the production of uniform binary oxides, the large differences in hydrolysis rates of different precursors can lead to undesirable inhomogeneities in the product. This is true of binary oxides derived from the transition metal alkoxides, especially those of d^0 transition metals, *e.g.* titanium and zirconium, which are widely used precursors for glasses and ceramics. The lower electronegativities of the transition metals compared to silicon make their alkoxides more reactive towards nucleophilic reactions such as hydrolysis and condensation.

One possible route to avoiding this complication is the non-hydrolytic sol–gel process, which is based on an observation made by Gerrard *et al.*[8] Whilst studying the interactions between organosilanes and alcohols, Gerrard *et al.* found silica to be formed. Since then, this route has been adapted to involve the direct condensation of metal halides with metal alkoxides, *e.g.* silicon, titanium and zirconium (Scheme 1).[9] The mechanism for this reaction involves the coordination of the oxygen donor, *e.g.* alkoxide, to the metal centre of the metal halide. This usually evolves *via* three possible transition states or intermediates and results in the formation of oxo-bridges. The non-hydrolytic route involves the cleavage of the carbon–oxygen bond instead of the metal–oxygen bond. The main limitation of this process is the insolubility of some metal chlorides in non-aqueous solvents. It also has a general tendency to delay crystallisation of the metal oxide. This process appears to be simpler to control than the conventional hydrolysis–condensation process found in the hydrolytic route. Mechanistically, the non-hydrolytic route should favour the formation of homogeneous binary oxides from different 'metal' precursors since the reaction of $M(OR)_m$ with $M'X_n$ should form unsymmetrical $M{-}O{-}M'$ linkages in the absence of reversibility and ligand exchange reactions. Another way to make non-hydrolytic sol–gels is to form the alkoxy groups *in situ*, by reacting the metal halide with an alcohol[10] or other organic oxo-compounds, *e.g.* ethers, aldehydes and ketones.[11]

The non-hydrolytic route has been used to make non-metal oxides, metal oxides, transition metal oxides and binary oxides, with the outstanding contribution coming from the group of Corriu.[12] Non-metal oxides, *e.g.* silica gels, have been studied most extensively. Stoichiometric reactions between silicon tetrahalides and various oxygen donors including alcohols, benzaldehyde and tetrabenzyloxysilane, have been examined.[13] Overall, alcohols appear to be more efficient oxygen donors than alkoxides, ethers and aldehydes. In the case of metal oxides, alumina gels have been studied by Corriu *et al.*, who found solvents to be necessary.[9,14] The main oxygen donors to aluminium halides were aluminium isopropoxide and diisopropyl ether. The alumina obtained was amorphous up to 750 °C compared to those obtained *via* the hydrolytic route which usually crystallise below 500 °C. As the precursors to the transition metal oxides are mostly liquids, these reactions often proceed without the need for solvents. Some of the oxygen donors used with titanium tetrachloride include tetrahydrofuran (THF), diisopropyl ether, dimethoxyethane (DME), and titanium isopropoxide.[9,15] Gel-times were longer than under hydrolytic conditions, which may be an advantage for titanium since this increases the potential for more control of the reaction. Other metal halides investigated include niobium, molybdenum and tungsten chlorides, but these lead to precipitates rather than gels. More recently, Guenther *et al.* reacted zirconium chloride with diisopropyl ether.[16] Further work by our group on single inorganic oxides prepared by the non-hydrolytic sol–gel route is reported separately.[17]

The rate of condensation in the non-hydrolytic process is highly dependent on the nature of the oxygen donor. The general tendency of the non-hydrolytic process compared to the hydrolytic route is to delay crystallisation[18] and this behaviour may find application in the preparation of heterogeneous catalysts. Different metals may also be used to form monolithic binary mixed metal oxides *via* a cross-condensation reaction (Scheme 2).[18–21]

The hydrolytic route to mixed metal oxides often leads to difficulties in controlling stoichiometry and homogeneity. Homogeneity depends on the rate of homocondensation (*i.e.* formation of $M{-}O{-}M$ and $M'{-}O{-}M'$) *versus* the rate of

---

† E-mail: j.hay@surrey.ac.uk

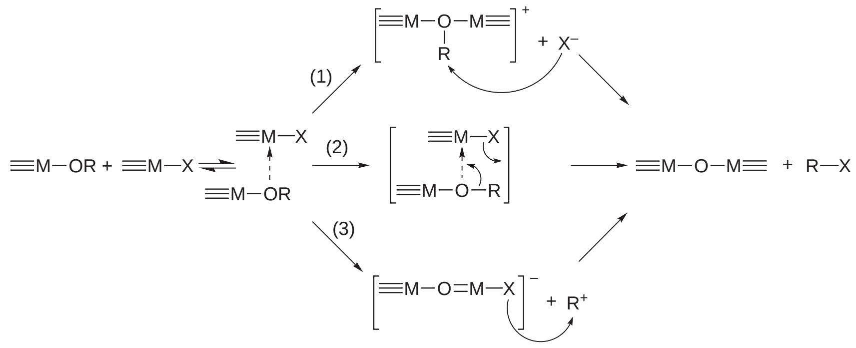

Scheme 1

$$m\mathrm{MX}_n + n\mathrm{M'(OR)}_m \longrightarrow \mathrm{M}_m\mathrm{M'}_n\mathrm{O}_{nm} + nm\mathrm{RX}$$

Scheme 2

heterocondensation (*i.e.* formation of M—O—M′). One way to overcome this in the hydrolytic route is to subject the less reactive alkoxide precursor to partial hydrolysis before adding the more reactive one, or to use heterometallic alkoxides. In principle, the non-hydrolytic process potentially provides a better route to mixed metal oxides than the conventional hydrolytic sol–gel approach or mixed powder methods because of improved homogeneity during the reaction.[22] This is in part a consequence of the reaction mechanism, which is completely different from that of the classical sol–gel process. As in the hydrolytic route, the reactants react at low temperature in a homogeneous solution or liquid, thus avoiding phase separation, crystallisation and chemical decomposition. Different combinations of silicon, aluminium and titanium chloride have been reacted with the corresponding isopropoxides.[9,18,20] In all cases gels were formed. Compositions can be controlled *via* the composition of starting solutions, since the results show that calcined gels are close in composition to initial solutions and this agrees with the high yields achieved. Iwasaki *et al.* have recently described the condensation of silicon tetraacetate with titanium acetylacetonatotriisopropoxide in THF.[23] More recently, it has been demonstrated that homogeneous zirconium titanate gels can be prepared by the non-hydrolytic sol–gel route without the intermediate formation of zirconia or titania.[21] In this paper we describe the synthesis and characterisation of further binary inorganic oxides *via* the solvent-free non-hydrolytic sol–gel route. To date, there are relatively few reports of the solvent-free synthesis of binary oxides by the sol–gel route, which is likely to be a prerequisite for the successful commercial development of products prepared by this method.

Experimental

Materials

Silicon tetrachloride (Aldrich), tetraethylorthosilicate, TEOS (Lancaster), aluminium trichloride (Aldrich), aluminium isopropoxide (Aldrich), titanium tetrachloride (Aldrich), titanium isopropoxide (Lancaster), ethanol (Hayman Ltd.) and iron(III) chloride (Aldrich) were all used as received. Propan-2-ol (Fisons), diethyl ether (Fisons) and carbon tetrachloride (BDH) were dried using 4 Å molecular sieves before use.

Method

Many of the materials used to make non-hydrolytic sol–gels are very reactive and have strict handling conditions. As a consequence, care should be taken when embarking on new and untried experiments, particularly in the absence of a diluting solvent. The basic set-up used in these experiments involved a reflux system, immersed in a temperature controlled oil bath, connected to a series of nitrogen drying vessels. A side arm was included above the reaction tube to allow the safe addition of air-sensitive liquid reactants from a syringe *via* a septum.

Instrumentation

A Shimadzu thermogravimetric analyser-50 was used to determine sample mass loss over a temperature range of 25–490 °C. A heating rate of 20 K min^{-1} was applied under a nitrogen atmosphere (flow rate, 50 ml min^{-1}). For mass losses up to higher temperatures, a Perkin-Elmer TGA-7 interfaced with a Perkin-Elmer 7700 computer was used to measure sample mass loss over a temperature range of 40–900 °C. A heating rate of 10 K min^{-1} was applied under a nitrogen atmosphere with a flow rate of 50 ml min^{-1}.

All calcinations were carried out in a Lenton UAF 16/21 furnace. An SMC 24127 calibrated digital K-type thermometer was used to control temperatures to ± 5 °C and the sample was contained in a mullite tube during the heating run. A Siemens D500 X-ray diffractometer was used to determine sample morphology. Samples were ground into fine powders before being scanned with Cu-Kα radiation at 40 kV, 40 mA from 15–70° 2θ, with a step size of 0.02° and a count time per step of 10 seconds. Surface morphology and evidence of any microporosity in the samples were evaluated using a CAMSCAM S4 field emission scanning electron microscope with an accelerating voltage of 5 kV for the secondary electron imaging (SEI) and 20 kV for the energy dispersive X-ray (EDX) analyses. Prior to mounting, the specimens were carbon coated to prevent charging under the electron beam. EDX spectra were acquired from a number of areas to determine the elemental composition of the sample.

Infrared (IR) spectra were recorded on a Perkin-Elmer 1750 FT-IR spectrophotometer interfaced with a Perkin-Elmer computer. Samples were ground and prepared for diffuse reflectance infrared Fourier transform spectroscopy (DRIFTS). Abbreviations used to describe peaks are as follows: vs = very strong; s = strong; m = medium; w = weak; vw = very weak; b = broad; sp = sharp and sh = shoulder.

Solid-state ^{29}Si nuclear magnetic resonance (NMR) spectroscopy was undertaken at the University of Durham, at ambient temperature on a Varian UNITY*plus* spectrometer. The spectrum was recorded against an external TMS standard with magic angle spinning (MAS) at a spinning rate of 4300 Hz and an angle of 54.7°. The cross polarised (CP) spectrum was obtained as a single contact experiment with a contact time of 3 ms and a relaxation delay of 2.0 s (700 repetitions). An acquisition time of 9.6 ms was used. Silicon sites were labelled with the conventional Q^n notation where Q refers to tetrafunctional $\mathrm{SiO_4}$ units and n to the number of bridging oxygen atoms surrounding the central silicon atom.

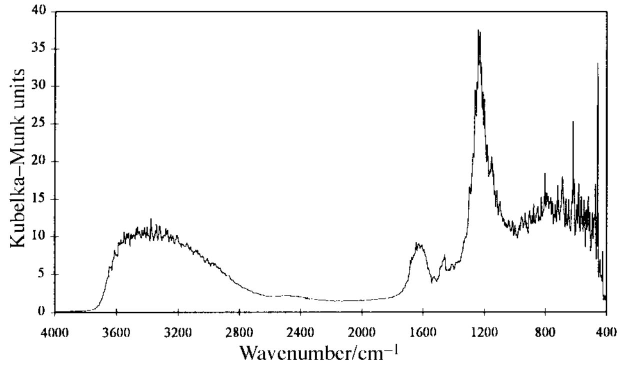

Fig. 1 FTIR spectrum of aluminosilicate synthesised from silicon tetrachloride and aluminium isopropoxide (equimolar)

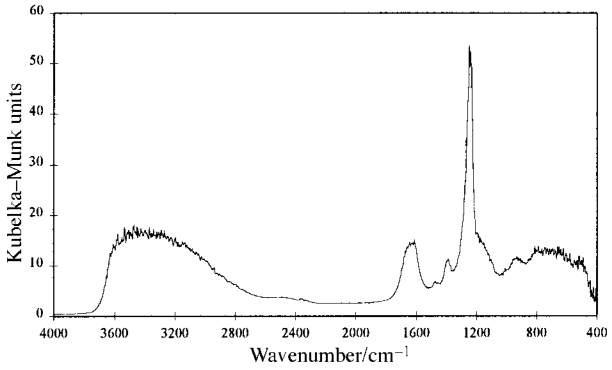

Fig. 2 FTIR spectrum of aluminosilicate synthesised from aluminium trichloride and TEOS (4:3 molar ratio)

Synthesis of binary oxides

Preparation of aluminosilicate from silicon tetrachloride and aluminium isopropoxide (equimolar) with the aid of a solvent. An equimolar amount of silicon tetrachloride (4.00 g, 2.70 cm^3, 0.024 mol) was added to aluminium isopropoxide (4.81 g, 0.024 mol) dissolved in a 4:1 (by mass) mixture of carbon tetrachloride and diethyl ether (4 cm^3). A white solid was formed within approximately 40 minutes at 90 °C. This was washed in propan-2-ol and dried for 3 days at 90 °C followed by a further 2 days at 150 °C (2.13 g, 81% yield based on $SiAlO_{3.5}$. Note: since the non-condensed sites of the network cannot be evaluated, yields are only included as information). The thermogravimetric analysis (TG) showed a mass loss of 14%. The IR spectrum (Fig. 1) showed absorptions at $\nu_{max} \approx 3400$ cm^{-1} (m, b), 1630 cm^{-1} (m), 1200 cm^{-1} (vs, sp), 1150 cm^{-1} (sh) and 450 cm^{-1} (vs, sp).

Preparation of aluminosilicate from aluminium trichloride and TEOS (equimolar) with the aid of a catalyst. Equimolar amounts of aluminium trichloride (2.06 g, 0.015 mol) and TEOS (3.12 g, 3.35 cm^3, 0.015 mol) were reacted with iron(III) chloride (0.070 g, *ca.* 1% by mass). A solid product was obtained within 3.5 hours at 110 °C. The solid was washed with ethanol and subsequently dried at 90 °C for 3 days and at 150 °C for a further 2 days (1.50 g, 84% yield based on $AlSiO_4$). The resulting monolith was dark brown in colour probably due to trapped catalyst. The TG showed 9% mass loss and the IR spectrum showed absorptions at $\nu_{max} \approx 3600$ cm^{-1} (b), 1600 cm^{-1} (vs, sp), 1250 cm^{-1} (m, sh), 1000 cm^{-1} (s, b), 950 cm^{-1} (sh) and 450 cm^{-1} (m).

Preparation of aluminosilicate from aluminium trichloride and TEOS (stoichiometric) with the aid of a catalyst. Aluminium trichloride (3.06 g, 0.023 mol) and TEOS (3.52 g, 3.76 cm^3, 0.017 mol) were mixed together in the presence of iron(III) chloride (0.068 g, 1.03% by mass). A clear, dark brown monolith was formed after approximately 10 minutes at 90 °C. The product was washed in diethyl ether (left overnight), filtered and dried at 150 °C for 3 days (2.08 g, 94% yield based on $Si_3Al_4O_{12}$). TG showed a 22% mass loss and the IR spectrum (Fig. 2) showed absorptions at $\nu_{max} \approx 3400$ cm^{-1} (m, b), 1611 cm^{-1} (m), 1250 cm^{-1} (s, sp), 1160 cm^{-1} (sh), 950 cm^{-1} (m), 800 cm^{-1} (m) and 500 cm^{-1} (m).

The dark brown and black coloured product of this reaction was calcined in air at 1000 °C for 18 hours, resulting in approximately 30% mass loss. The resulting specimen was heterogeneously coloured black, brown and off-white. The X-ray diffraction (XRD) pattern of the oxide prior to calcination and that after calcination are shown in Fig. 3. The latter shows a very good fit with an orthorhombic mullite structure, $Al_6Si_2O_{13}$, with no crystalline peaks left unmatched. The scanning electron micrograph (SEM) showed this material to be highly porous, with the pores being approximately 200 nm in diameter. EDX analysis of the bulk material (Fig. 4) showed the elements aluminium, silicon and oxygen. Iron was also present in some loose material covering the surface of the sample. The IR spectrum (Fig. 5) showed absorptions at $\nu_{max} \approx 3600$ cm^{-1} (vw), 2000 cm^{-1} (vw), 1880 cm^{-1} (w), 1620 cm^{-1} (w), 1330 cm^{-1} (vs, sp), 1240 cm^{-1} (m), 1030 cm^{-1} (m), 930 cm^{-1} (m), 850 cm^{-1} (s), ~640 cm^{-1} (s), 529 cm^{-1} (s) and 420 cm^{-1} (m).

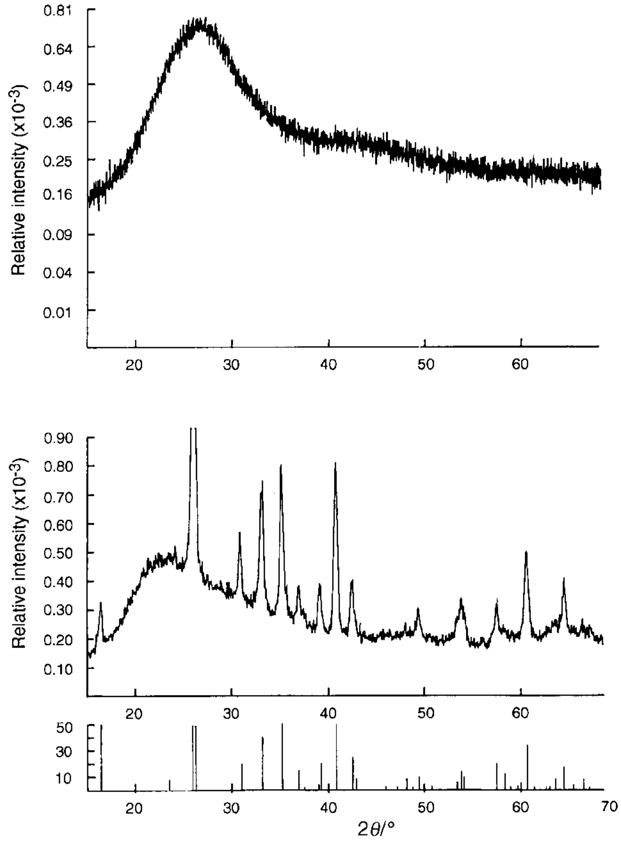

Fig. 3 XRD spectrum of aluminosilicate prior to calcination (top) and after calcination (below) at 1000 °C for 18 hours accompanied by the peak positions observed for $Al_6Si_2O_{13}$

Preparation of titanium–silicon binary oxide from silicon tetrachloride and titanium isopropoxide (equimolar).[18–21] Equimolar amounts of silicon tetrachloride (2.00 g, 1.35 cm^3, 0.012 mol) and titanium isopropoxide (3.35 g, 3.5 cm^3, 0.012 mol), were reacted at 55 °C. A fine white precipitate was seen within 1 minute of stirring at room temperature and this disappeared at approximately 45 °C. A clear, pale brown, crazed solid resulted in less than 24 hours and was washed in

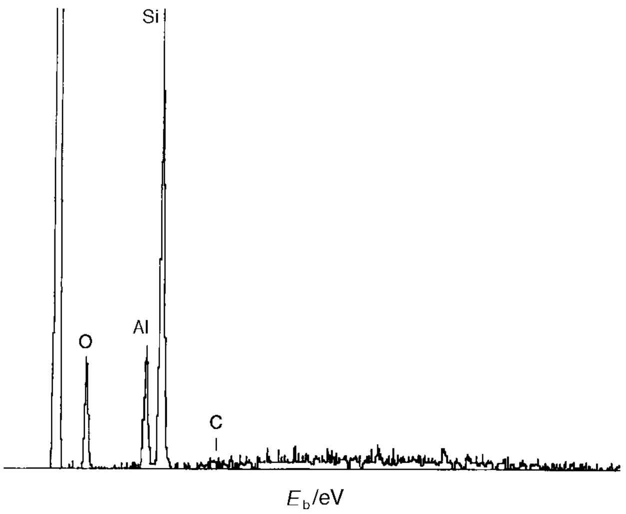

Fig. 4 EDX spectrum of aluminosilicate calcined for 18 hours at 1000 °C (bulk)

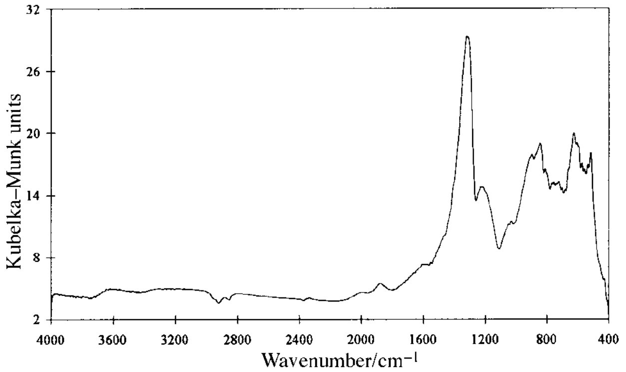

Fig. 5 FTIR spectrum of aluminosilicate calcined for 18 hours at 1000 °C

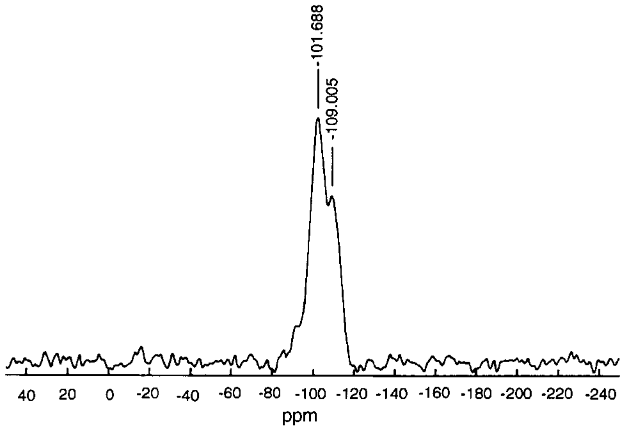

Fig. 6 ^{29}Si NMR spectrum of titanium–silicon binary oxide prior to calcination

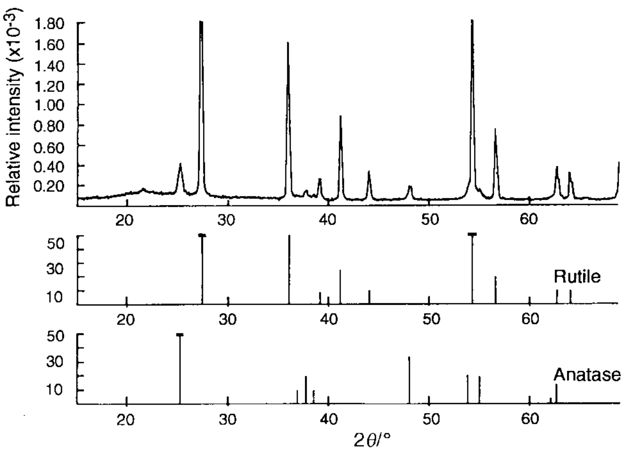

Fig. 7 XRD spectrum of titanium–silicon binary oxide calcined for 18 hours at 1000 °C accompanied by the peak positions observed for rutile and anatase

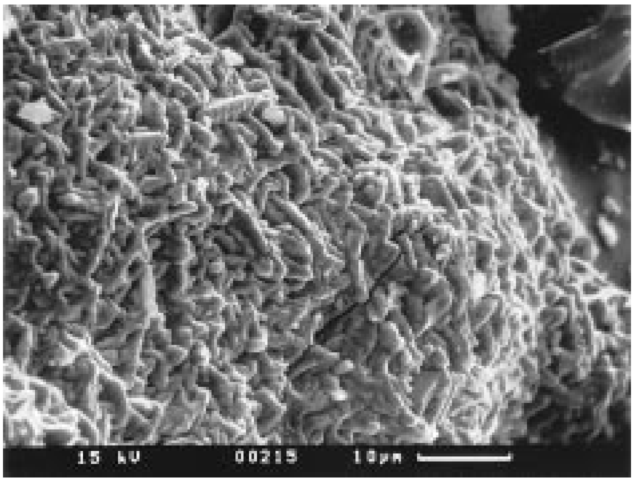

Fig. 8 SEM of titanium–silicon binary oxide calcined for 18 hours at 1000 °C

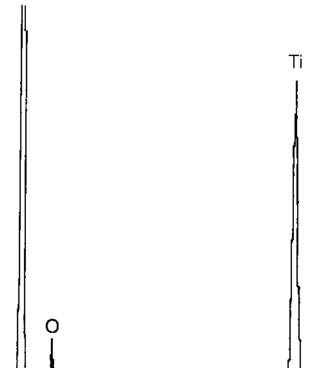

Fig. 9 EDX spectrum of titanium–silicon binary oxide calcined for 18 hours at 1000 °C (bulk)

propan-2-ol and dried at 85 °C for 2 hours producing a creamy, shell-like product (1.70 g, 101% yield based on $TiSiO_4$). TG showed a 20% mass loss. When subjected to further drying at 140 °C for 24 hours, a charcoal black solid was formed (1.36 g, 81% yield). The IR spectrum shows absorptions at $\nu_{max} \approx 3500$ cm^{-1} (s, b), 1630 cm^{-1} (m), ~1100 cm^{-1} (s, b) and 600 cm^{-1} (s, b). The ^{29}Si NMR spectrum is shown in Fig. 6.

The black material was calcined in air at 1000 °C for 18 hours to leave a white solid (≈28% mass loss). A thin black coating covered the surface of a few particles. Qualitative XRD results (Fig. 7) show a good fit with two titania phases; tetragonal rutile and anatase. There seemed to be more rutile than anatase present, but no silica phase was detected. A typical SEM is shown in Fig. 8. The EDX spectrum (Fig. 9) showed the bulk of the specimen to have a high titanium content in addition to the silicon and oxygen signals.

Preparation of titanium–silicon binary oxide from titanium tetrachloride and TEOS (equimolar). An equimolar amount of titanium tetrachloride (4.00 g, 2.32 cm^3, 0.021 mol) was reacted with TEOS (4.39 g, 4.70 cm^3, 0.021 mol) for 5 minutes at 110 °C. The dark brown gel was washed in ethanol, filtered and dried at 150 °C for 4 days (3.66 g, 124% yield based on $TiSiO_4$). TG showed a 28% mass loss and the IR spectrum showed absorptions at $\nu_{max} \approx 3500$ cm^{-1} (m, b), ~ 3000 cm^{-1} (m), 1850 cm^{-1} (vw, b), 1630 cm^{-1} (m, sp), 1430 cm^{-1} (m, sp), 1370 cm^{-1} (m, sp), 1250 cm^{-1} (vs, sp), 1160 cm^{-1} (s), 960 cm^{-1} (m), 810 cm^{-1} (m) and 525 cm^{-1} (m).

Preparation of titanium–aluminium binary oxide from aluminium trichloride and titanium isopropoxide (4 : 3 molar ratio). An appropriate stoichiometric amount of aluminium trichloride (2.00 g, 0.015 mol) was reacted with titanium isopropoxide (3.20 g, 3.35 cm^3, 0.011 mol) for 24 hours at 110 °C. The dark brown monolith was washed in diethyl ether (left overnight), filtered and dried for 3 days at 150 °C (1.88 g, 113% yield based on $Al_4Ti_3O_{12}$). TG showed a 26% mass loss. The IR spectrum produced absorptions at $\nu_{max} \approx 3400$ cm^{-1} (s, b), 1630 cm^{-1} (vs, sp), 1100 cm^{-1} (s), ~ 900 cm^{-1} (vs, b), 800 cm^{-1} (s) and 600 cm^{-1} (m, b).

Preparation of titanium–aluminium binary oxide from titanium tetrachloride and aluminium isopropoxide (3 : 4 molar ratio). Appropriate stoichiometric amounts of titanium tetrachloride (4.00 g, 2.32 cm^3, 0.021 mol) and aluminium isopropoxide (5.74 g, 0.028 mol) were stirred together for approximately 6 hours at 110 °C. The dark brown sample was washed with propan-2-ol and then dried for 4 days at 150 °C leaving a black shiny material (4.59 g, 147% yield based on $Ti_3Al_4O_{12}$). TG showed a 35% mass loss. The IR spectrum showed absorptions at $\nu_{max} \approx 3500$ cm^{-1} (m, b), 3000 cm^{-1} (m, sh), 1630 cm^{-1} (m), 1100 cm^{-1} (s), 1000 cm^{-1} (vs, sp), 800 cm^{-1} (m, sh) and ~ 450 cm^{-1} (w).

Results and Discussion

Aluminium–silicon oxides

Three experiments were undertaken on the synthesis of aluminosilicates similar to those reported by Corriu *et al.*[19] A solvent was employed for the initial reaction to moderate the potentially vigorous reaction between silicon tetrachloride and aluminium isopropoxide. A stoichiometric ratio of 1 : 1 was used, compared to the halide to alkoxide ratio of 1 : 4/3 used by Corriu *et al.* Use of a higher reaction temperature in our case led to rapid formation of the initial product, compared to a literature gel-time of two days at 40 °C. The IR spectrum (Fig. 1) of the white product confirmed the formation of aluminosilicate.[24] The presence of a band at ≈ 1200 cm^{-1} may be indicative of aluminium substitution in the silica network. The peak at ≈ 1150 cm^{-1} appears as a shoulder and can be assigned to the elongation vibration of Si—O—Al. Vibrations between 3500–3400 cm^{-1} and at 1630 cm^{-1} are due to the stretching of hydroxyl groups from either hydrogen bonded water or propan-2-ol and surface silanol molecules. The latter absorption is due to the deformation mode of these hydroxyl groups. The TG indicated an incomplete reaction, probably due to the presence of unreacted material and trapped solvent or by-product.

No solvent was used for the reaction of aluminium trichloride with TEOS; however, based on studies by Corriu *et al.*,[25] a catalyst was employed in the reactions to reduce reaction times and residual unreacted functionalities. Two ratios were studied. At a 1 : 1 ratio of aluminium halide to TEOS, a good yield was achieved after 3.5 hours at 110 °C, with a relatively small TG mass loss due to residual volatiles, implying good oxide conversion. The IR analysis[24] suggested aluminosilicate formation. At a 4 : 3 molar ratio of aluminium trichloride to TEOS, a shorter gel-time was achieved at a lower temperature and the yield was the highest of the aluminosilicate sol–gel systems; however, the TG showed a higher percentage mass loss, suggesting incomplete reaction. IR analysis (Fig. 2) was indicative of formation of a binary oxide, which might be expected to have the empirical formula $Al_4Si_3O_{12}$ on the basis of the stoichiometry (Scheme 3).

$$4\,AlCl_3 + 3\,Si(OC_2H_5)_4 \xrightarrow{FeCl_3} Al_4Si_3O_{12} + 12\,C_2H_5Cl$$

Scheme 3

The XRD pattern of the oxide prior to calcination (Fig. 3) shows the sample to be amorphous with a broad peak at the low angle end of the spectrum. Following calcination of the oxide at 1000 °C, XRD analysis reveals that the sample has crystallised, although an amorphous phase is still present. The XRD trace shows a very good fit with an orthorhombic mullite structure, $Al_6Si_2O_{13}$, with no peaks left unmatched. The stoichiometry of this structure is very different to that expected from the reaction stoichiometry and may result from the presence of an amorphous silica phase in the calcined structure. The extent to which molecular or network rearrangement has occurred during the calcination process is impossible to ascertain from these results. It should be noted that at 1000 °C, the thermodynamics control the crystallisation process of the mullite. The possibility of nucleation initiated by the mullite tube used in the calcination can not be totally discounted. Optimisation of the reaction stoichiometry might maximise formation of a crystalline mullite after calcination, but this was not carried out as part of this study. Longer heating times might also improve the conversion.

The SEMs show the calcined product to be highly porous, with pores of approximately 200 nm diameter. The sample surface was covered with loose material which, using EDX analysis, was found to contain a high iron content (catalyst residue) in addition to the elements aluminium, silicon and oxygen which were found in the EDX spectrum of the bulk material (Fig. 4). The aluminium signal is much weaker than the silicon signal, in contrast to the Al : Si ratio of 6 : 2 found for the crystalline phase using XRD analysis. This apparent discrepancy may be explained by the fact that XRD analysis provides information only on the crystalline phase, while EDX analysis averages the analysis of the bulk sample, including amorphous material (such as silica). An additional factor may be the influence of the surface roughness of the sample on the consistency of the quantitative analyses obtained by EDX. Following calcination, IR analysis showed that the siloxane stretching vibration at ≈ 1180 cm^{-1} had disappeared and been replaced by a higher frequency band at 1330 cm^{-1} (Fig. 5), which could result from crystallisation of the aluminosilicate.

Titanium–silicon oxides

For the titanium–silicon binary oxide system prepared from silicon tetrachloride and titanium isopropoxide, the results tend to agree with published findings on related systems.[19] IR spectroscopy provides limited evidence for the presence of Ti—O—Si species in the initial amorphous product. Solid-state ^{29}Si NMR spectroscopy was used to obtain data on the extent of Ti—O—Si bonding in the system (Fig. 6). The spectrum shows the expected Si—O—Si signals at -101 ppm and -109 ppm. These were assigned to partially condensed, Q^3 ($ROSiO_3$) species and fully condensed, Q^4 (SiO_4) species. No signals (expected at ≈ -20 ppm) could be attributed to the presence of Ti—O—Si species,[26] suggesting the product was actually a phase separated mixture of silica and titania. The poor stability of Ti—O—Si bonds may help to explain this result since any first-formed Ti—O—Si species will rearrange on ageing to form Si—O—Si and Ti—O—Ti species. The XRD pattern (Fig. 7) verified that after calcination at 1000 °C, the majority of the sample had crystallised. A good fit was obtained with two titania phases, tetragonal rutile and anatase with more of the former present. No crystalline silica was detected, although other studies undertaken by us had shown that pure silica formed by the non-hydrolytic sol–gel process could by crystallised under similar calcination conditions to form mixtures of quartz and cristobalite.[17] Some possible reasons for this are: (a) the 'silica' is actually present as a genuine titanium–silicon hybrid oxide which does not crystallise under these conditions, or (b) the phase size of the silica is too small for crystallisation to occur in this system—a recent study has demonstrated that there is a strong size dependence of crystallisation kinetics in inorganic nanocrystals.[27] NMR evidence showing the absence of Ti—O—Si species in the original amorphous product suggests rationale (b) may be the most reasonable explanation for the failure of the silica to crystallise.

Corriu *et al.*[18–21] calcined a similar titanium–silicon oxide at 500 °C for five hours. They also detected no silica *via* XRD analysis, only crystallites of anatase. No rutile was found. Elemental analysis of the oxide showed it to be practically carbon-free and have a metal content very close to the composition of the starting solution. The microchemical analytical study by means of an electron-probe analyser, *i.e.* energy-dispersive spectroscopy, indicated a constant Ti : Si ratio (close to unity), which is consistent with homogeneity at the micrometer level. Analysis of our sample *via* EDX (Fig. 9) agreed qualitatively with this finding. Homogeneity on an atomic scale would lead to a true binary oxide on crystallisation instead of a mixture of individual oxides (TiO_2 and SiO_2); however, the empirical formula predicted for our product is $TiSiO_4$ which is not a known compound.[22] For pure titania systems synthesised *via* the non-hydrolytic route, Corriu *et al.*[15] concluded that compared to the conventional sol–gel route,[28] the crystallisation of titania is delayed as is the anatase to rutile transformation.[29] In our titanium–silicon system, the XRD results show that crystallisation of titania phases, in particular rutile, is the primary crystallisation process, with no evidence for formation of a crystalline binary oxide.

The low magnification SEM shows the general, crazed morphology of the surface of this oxide. Again, a lot of loose material is present. At a higher magnification, the faceted nature of the crystallites is highlighted (Fig. 8). The EDX spectrum (Fig. 9) shows the presence of both silicon and titanium as well as oxygen.

For the reaction of TEOS with titanium tetrachloride, no catalyst was necessary owing to the high reactivity of the transition metal halide. At 110 °C, this reaction reached gelation rapidly. The TG result suggested that the high yield obtained was due to the presence of unreacted precursors. The IR spectrum suggested binary oxide formation, with a Si—O—Ti stretching vibration at 960 cm^{-1} in addition to Ti—O—Ti elongation bands[30] at 1250 cm^{-1} and 725 cm^{-1} and Si—O—Si stretching absorption bands[2,31,32] at 1220 cm^{-1}, 810 cm^{-1} and 525 cm^{-1}. Corriu *et al.*[19] have performed a similar reaction but used silicon isopropoxide instead of TEOS. They formed a gel in five days at 40 °C, with a 100% oxide yield. A 10% mass loss was seen up to 1200 °C. XRD, determined after five hours heat treatment of their product at 500 °C, showed the crystalline phase to be anatase and the specific surface area, also after calcination at this temperature, was found to be 590 m^2 g^{-1}. In the reaction between titanium tetrachloride and TEOS, the condensation rate needs to be reduced in order to achieve greater reaction control, *i.e.* by reducing the reaction temperature a lower reaction rate would avoid premature gelation and improve precursor mobility. This should improve the homogeneity of the two components and consequently allow the reaction to proceed further towards completion.

$$3\,Ti(OPr^i)_4 + 4\,AlCl_3 \longrightarrow Ti_3Al_4O_{12} + 12\,Pr^iCl$$

Scheme 4

$$3\,TiCl_4 + 4\,Al(OPr^i)_3 \longrightarrow Ti_3Al_4O_{12} + 12\,Pr^iCl$$

Scheme 5

Titanium–aluminium oxides

Two complementary experiments were carried out to investigate the formation of titanium–aluminium binary oxides. The first is the reaction of aluminium trichloride with titanium isopropoxide (Scheme 4) and the second the reverse reaction of titanium tetrachloride with aluminium isopropoxide (Scheme 5). In the first reaction between aluminium trichloride and titanium isopropoxide, the TG result confirms that the high yield obtained was most likely due to trapped solvent or by-product. The IR spectrum was difficult to interpret. In the absence of literature data on the assignment of titanium–aluminium binary oxide peaks, all that can be deduced is general oxide formation. The second reaction appeared to be even more incomplete. The yield achieved was very high and the TG mass loss supported this result. The IR spectrum was also difficult to interpret. All that can be deduced is oxide formation, with Al—O absorptions[24] at 1100 cm^{-1} and 800 cm^{-1}. A slight shift to a higher frequency in the tentatively assigned Ti—O stretching band at ≈1000 cm^{-1} might indicate Al—O substitution.[30] Longer reaction times are undoubtedly required to force the titanium–aluminium reactions to completion and much more work would be needed to fully characterise the products. This was not justified in the context of the present work.

Conclusions

The non-hydrolytic sol–gel route to inorganic oxides has been extended to the synthesis of a series of binary oxides based on silicon, aluminium and titanium. In principle, one advantage of this route over the well established hydrolytic route is that reactivity differences between different 'metals' are reduced, therefore offering the promise of more homogeneous binary systems. Since many of the starting inorganic halides and alkoxides are liquids, this offers the prospect of carrying out the reactions under solvent-free conditions, albeit paying due respect to the high reactivity of some of these systems! Binary systems based on aluminium–silicon, titanium–silicon and titanium–aluminium combinations were studied.

As expected, reactions were generally rapid in the absence of a solvent and the presence, where necessary, of a catalyst [iron(III) chloride]. Formation of true aluminosilicates was demonstrated, although in one case it was shown by XRD that the crystalline product resulting from calcination had a structure (mullite) different from that expected solely from the reaction stoichiometry. The extent to which this resulted from network rearrangement processes during calcination was not determined. At the calcination temperature of 1000 °C, thermodynamics control the crystallisation of mullite. Amorphous material such as silica was also present. In the case of titanium–silicon systems, there was no clear spectroscopic evidence for the initial formation of a binary oxide. The results after calcination showed the presence of only pure crystalline titania phases. The presence of silica nanophases could explain the lack of silica crystallisation under these conditions. In the case of the titanium tetrachloride/TEOS reaction, a lower reaction rate might improve product homogeneity. The titanium–aluminium reactions led to incomplete oxide formation and unequivocal evidence for binary oxide formation was not obtained. Further optimisation of the reaction conditions and more in-depth analysis of the products are required to demonstrate the potential for binary oxide formation in these systems.

Overall, this study has shown that in the silicon, aluminium, titanium series, amorphous binary oxides can in some cases be formed directly *via* the non-hydrolytic sol–gel reaction, but only the aluminosilicates appear to form true crystalline binary oxides after calcination at 1000 °C. Optimisation of the initial reaction conditions and/or stoichiometry may lead to improved homogeneity in the other systems.

The authors are grateful to the Engineering & Physical Sciences Research Council (EPSRC) and the Defence, Evaluation & Research Agency (DERA) for the award of a CASE studentship (to H. R.). We also thank DERA for use of their facilities and for undertaking XRD and SEM analyses. Particular thanks are due to Dr M. Clegg and Dr D. Porter (both DERA) for helpful discussions and suggestions. We also thank the University of Durham for provision of solid state ^{29}Si NMR services.

References

1 C. L. Bird and A. T. Kuhn, *Chem. Soc. Rev.*, 1981, **10**, 49.
2 C. J. Brinker and G. W. Scherer, *The Physics and Chemistry of Sol–Gel Processing*, Academic Press, London, 1990.
3 D. Avnir, *Acc. Chem. Res.*, 1995, **28**, 328.
4 B. M. Novak, *Adv. Mater.*, 1993, **5**, 422.
5 J. Livage *et al.*, *Prog. Solid State Chem.*, 1988, **18**, 259.
6 C. D. Chandler, C. Roger and M. J. Hampden-Smith, *Chem. Rev.*, 1993, **93**, 1205.
7 L. Hench and J. K. West, *Chem. Rev.*, 1990, **90**, 33.
8 W. Gerrard and P. F. Griffet, *Chem. Ind.*, 1959, 55.
9 (*a*) S. Acosta, P. Arnal, R. J. P. Corriu, D. Leclercq, P. H. Mutin and A. Vioux, *Mater. Res. Soc. Symp. Proc.*, 1994, **346**, 43; (*b*) R. J. P. Corriu, D. Leclercq, P. Lefèvre, P. H. Mutin and A. Vioux, *J. Mater. Chem.*, 1992, **2**, 673; (*c*) R. J. P. Corriu, D. Leclercq, P. Lefèvre, P. H. Mutin and A. Vioux, *J. Sol-Gel Sci. Technol.*, 1997, **8**, 89.
10 (*a*) W. Gerrard and J. V. Jones, *J. Chem. Soc.*, 1952, 1690; (*b*) W. Gerrard and K. D. Kilburn, *J. Chem. Soc.*, 1956, 1536.
11 (*a*) A. Zappel, *J. Am. Chem. Soc.*, 1955, **77**, 4228; (*b*) R. Schwartz and W. Kucher, *Chem. Ber.*, 1956, **89**, 169.
12 (*a*) R. J. P. Corriu and D. Leclercq, *Angew. Chem., Int. Ed. Engl.*, 1996, **35**, 1420; (*b*) D. Leclercq and A. Vioux, *Heterog. Chem. Rev.*, 1996, **3**, 65.
13 R. J. P. Corriu, D. Leclercq, P. Lefèvre, P. H. Mutin and A. Vioux, *J. Non-Cryst. Solids*, 1992, **146**, 301.
14 S. Acosta, R. J. P. Corriu, D. Leclercq, P. Lefèvre, P. H. Mutin and A. Vioux, *J. Non-Cryst. Solids*, 1994, **170**, 234.
15 (*a*) P. Arnal, R. J. P. Corriu, D. Leclercq, P. H. Mutin and A. Vioux, *Mater. Res. Soc. Symp. Proc.*, 1994, **346**, 339; (*b*) P. Arnal, R. J. P. Corriu, D. Leclercq, P. H. Mutin and A. Vioux, *J. Mater. Chem.*, 1996, **6**, 1925.
16 E. Guenther and M. Jansen, *Chem. Mater.*, 1995, **7**, 2110.
17 J. N. Hay and H. M. Raval, *J. Sol-Gel Sci. Technol.*, in press.
18 (*a*) M. Andrianainarivelo, R. J. P. Corriu, D. Leclercq, P. H. Mutin and A. Vioux, *J. Mater. Chem.*, 1996, **6**, 1665; (*b*) M. Andrianainarivelo, R. J. P. Corriu, D. Leclercq, P. H. Mutin and A. Vioux, *Chem. Mater.*, 1997, **9**, 1098.
19 R. J. P. Corriu, D. Leclercq, P. Lefèvre, P. H. Mutin and A. Vioux, *Chem. Mater.*, 1992, **4**, 961.
20 S. Acosta, R. J. P. Corriu, D. Leclercq, P. H. Mutin and A. Vioux, *Mater. Res. Soc. Symp. Proc.*, 1994, 345.
21 M. Andrianainarivelo, R. J. P. Corriu, D. Leclercq, P. H. Mutin and A. Vioux, *J. Mater. Chem.*, 1997, **7**, 279.
22 H. Dislich, *Angew. Chem., Int. Ed. Engl.*, 1971, **10**, 363.
23 I. Iwasaki, S. Yasumroi, S. Shibata and M. J. Yamane, *Sol-Gel Sci. Technol.*, 1994, **2**, 387.
24 T. López, M. Asomosa, L. Razo and R. Gómez, *J. Non-Cryst. Solids*, 1989, **108**, 45.
25 L. Bourget, R. J. P. Corriu, D. Leclercq, P. H. Mutin and A. Vioux, in *First European Workshop on Hybrid Organic-Inorganic Materials*, ed. C. Sanchez and F. Ribot, Paris, 1993, **305**, 308.
26 (*a*) F. Babonneau, *New J. Chem.*, 1994, **18**, 1065; (*b*) P. Prasad and B. A. Reinhardt, *Chem. Mater.*, 1990, **2**, 660.
27 C.-C. Chen, A. B. Herhold, C. S. Johnson and A. P. Alivisatos, *Science*, 1997, **276**, 398.
28 (*a*) K. Kamiya, K. Tanimoto and T. Yoko, *J. Mater. Sci. Lett.*, 1986, **5**, 402; (*b*) M. Aizawa, Y. Nakagawa, Y. Nosaka, N. Fujii and H. Miyama, *J. Non-Cryst. Solids*, 1990, **124**, 112.
29 P. Arnal, R. J. P. Corriu, D. Leclercq, P. H. Mutin and A. Vioux, *Chem. Mater.*, 1997, **9**, 694.
30 M. Schraml-Marth, K. L. Walther and A. Wokaun, *J. Non-Cryst. Solids*, 1992, **143**, 93.
31 *Analysis of Silicones*, ed. A. L. Smith, Wiley-Interscience, New York, 1974.
32 R. K. Iler, *The Chemistry of Silica*, Wiley, New York, 1979.

Paper 7/07549I; *Received* 20*th October*, 1997